

# 1 **A metabolic CRISPR-Cas9 screen in Chinese hamster ovary** 2 **cells identifies glutamine-sensitive genes**

3

4 Karen Julie la Cour Karottki<sup>1</sup>, Hooman Hefzi<sup>2,4,5</sup>, Songyuan Li<sup>1</sup>, Lasse Ebdrup Pedersen<sup>1</sup>,  
5 Philipp Spahn<sup>2,4</sup>, Chintan Joshi<sup>2,4</sup>, David Ruckerbauer<sup>6,7</sup>, Juan Hernandez Bort<sup>6</sup>, Alex  
6 Thomas<sup>2</sup>, Jae Seong Lee<sup>8</sup>, Nicole Borth<sup>6,7</sup>, Gyun Min Lee<sup>3</sup>, Helene Faustrup Kildegaard<sup>1,\*</sup>,  
7 Nathan E. Lewis<sup>2,4,5,\*</sup>

8

9 <sup>(1)</sup> The Novo Nordisk Foundation Center For Biosustainability, Technical University Of Denmark, Denmark

10 <sup>(2)</sup> The Novo Nordisk Foundation Center For Biosustainability At The University Of California, San Diego, USA

11 <sup>(3)</sup> Department Of Biological Sciences, Kaist, 291 Daehak-Ro, Yuseong-Gu, Daejeon 305-701, Republic Of Korea

12 <sup>(4)</sup> Department of Pediatrics, University of California, San Diego, USA

13 <sup>(5)</sup> Department of Bioengineering, University of California, San Diego, USA

14 <sup>(6)</sup> Austrian Centre of Industrial Biotechnology, Vienna, Austria

15 <sup>(7)</sup> University of Natural Resources and Life Sciences, Vienna, Austria

16 <sup>(8)</sup> Department of Molecular Science and Technology, Ajou University, Suwon 16499, Republic of Korea

17 \* Equal contribution, Correspondence to: Nathan E. Lewis, [nlewisres@ucsd.edu](mailto:nlewisres@ucsd.edu)

18

19

20 **Keywords:** CHO, CRISPR pooled screen, glutamine, metabolism<sup>1</sup>

---

<sup>1</sup> **Abbreviations:**  $\alpha$ kgdhc - alpha ketoglutarate dehydrogenase complex; Cas9 – CRISPR-associated protein 9; CHO – Chinese hamster ovary; CPM - counts per million; CRISPR – clustered regularly interspaced short palindromic repeats; DAPI – 4',6-diamidino-2-phenylindole; GFP – green fluorescent protein; GLS - glutaminase; GLUL - glutamine synthetase; gRNA – guide RNA; Mgat1 - mannosyl (alpha-1,3-)- glycoprotein beta-1,2-N-acetylglucosaminyltransferase; NGS – next generation sequencing ; RNAi – RNA interference; TALEN - transcription activator-like effector nucleases; VCD – viable cell density; ZFN – zinc-finger nuclease

21  
22  
23  
24  
25  
26  
27  
28  
29  
30  
31  
32  
33  
34  
35  
36  
37  
38  
39  
40  
41

## Abstract

Over the past decades, optimization of media formulation and feeding strategies have fueled a many-fold improvement in CHO-based biopharmaceutical production. While Design of Experiments (DOE) and media screens have led to many advances, genome editing offers another avenue for enhancing cell metabolism and bioproduction. However the complexity of metabolism, involving thousands of genes, makes it unclear which engineering strategies will result in desired traits. Here we developed a comprehensive pooled CRISPR screen for CHO cell metabolism, including ~16,000 gRNAs against ~2500 metabolic enzymes and regulators. We demonstrated the value of this screen by identifying a glutamine response network in CHO cells. Glutamine is particularly important since it is often substantially overfed to drive increased TCA cycle flux but can lead to accumulation of toxic ammonia. Within the glutamine-response network, the deletion of a novel and poorly characterized lipase, *Abhd11*, was found to substantially increase growth in glutamine-free media by altering the regulation of the TCA cycle. Thus, the screen provides an invaluable targeted platform to comprehensively study genes involved in any metabolic trait.

42 Chinese hamster ovary (CHO) cells are the most commonly used mammalian cells for  
43 biotherapeutic protein production and serve as the expression system of choice for the leading  
44 biologics<sup>1</sup>. Consequently, improving product quality and decreasing manufacturing costs in  
45 CHO is of great interest to the biopharmaceutical industry. Since their first use in the late  
46 1980s, final product titers from CHO cells have improved more than 50-fold, largely through  
47 media and bioprocess optimization<sup>2</sup>. Although effective, these empirical approaches are highly  
48 variable, demand extensive labor, time, and resources, and may not translate directly to new  
49 clones.

50 All biological processes that lead to protein production depend on metabolic building  
51 blocks. Although CHO cell media are complex owing to their nutritional demands<sup>3</sup> the two  
52 main nutrients consumed are glucose and glutamine. These are often taken up in excess of the  
53 cells growth needs<sup>4</sup> leading to increased by-product formation of lactate and ammonia,  
54 respectively, which are the two primary byproducts negatively affecting cell growth,  
55 production and product quality<sup>5-8</sup>. The complexity and incomplete understanding of  
56 metabolism, along with unique idiosyncrasies of individual CHO clones have stymied the  
57 optimization of their metabolism. However, the release of CHO and Chinese hamster genome  
58 sequences<sup>9-11</sup> and improved systems biology approaches<sup>3,12</sup> have laid the groundwork for a  
59 new era of targeted CHO cell line development, but the question of the best way to discover  
60 and engineer targets remains open.

61 Several techniques can be used to knock out genes in CHO cells, such as zinc finger  
62 nucleases (ZFNs)<sup>13</sup>, transcription activator-like effector nucleases (TALENs)<sup>14</sup>, and Clustered  
63 Regularly Interspaced Short Palindromic Repeats (CRISPR). However, since the best genes to

64 knock out are often unclear, given >20,000 genes in the CHO genome, efficient, high-  
65 throughput methods are needed to identify optimal genetic modifications. Although RNA  
66 interference (RNAi) screening has been useful for identifying gene knockdowns<sup>15</sup> providing a  
67 desired trait in CHO cells<sup>16</sup>, the inability to achieve full knockout, a significant amount of off-  
68 target effects<sup>17</sup>, and inconsistent results has limited their use<sup>18</sup>. On the other hand, CRISPR-  
69 Cas9 can also be used for large-scale pooled screening while avoiding some of the pitfalls in  
70 RNAi screens<sup>19</sup>. The method has been established in several cell lines and organisms, mainly  
71 mouse and human, increasing the robustness for the next generation of forward genetic  
72 screening methods<sup>19–23</sup>.

73         With the intent of generating a platform for gaining insight into CHO cell metabolism,  
74 we present a large-scale CHO-specific CRISPR-Cas9 knockout screen in CHO cells. We  
75 generated a gRNA library targeting genes for enzymes and regulators involved in CHO cell  
76 metabolism. We deployed CRISPR-Cas9 knockout screening against an industrially relevant  
77 selection pressure, glutamine deprivation, and identified a network of genes regulating growth  
78 in response to glutamine concentration. We highlight one gene for a novel and poorly  
79 characterized lipase, *Abhd11*, which, upon deletion, we found to substantially increase growth  
80 glutamine-free media by altering the regulation of the TCA cycle.

81

## 82 **Results**

### 83 **Establishing a CRISPR knockout library in CHO cells**

84         We first generated CHO-S cell lines constitutively expressing Cas9 (CHO-SCas9) via  
85 G418 selection followed by single cell sorting and expansion to obtain clonal populations for

86 subsequent gRNA library transduction. We validated the functionality of Cas9 in the clonal  
87 cell lines by transfecting CHO-SCas<sup>9</sup> with a gRNA targeting *Mgat1* and quantifying the cleavage  
88 efficiency by indel analysis of the target region (Supplementary Table S1). To generate the  
89 CRISPR knockout library, we designed a large CHO-specific gRNA library containing 1-10  
90 gRNAs/gene for genes encoding enzymes and regulators of CHO metabolism. Genes selected  
91 for inclusion were obtained from the genome scale metabolic model of CHO<sup>3</sup>, metabolism-  
92 associated GO terms, and transcription factors that regulate the aforementioned genes (based  
93 on annotation from Ingenuity Pathway Analysis<sup>24</sup>). The library consists of 15,654 gRNAs  
94 against 2,599 genes (1,765 genes from the model, 782 from GO terms, and 52 transcription  
95 factors)(Supplementary Datafile 1). gRNAs were synthesized by CustomArray Inc. and  
96 subsequently packaged into lentiviruses. CHO-SCas<sup>9</sup> cells were then transduced with the gRNA  
97 library at low multiplicity of infection (MOI) (Supplementary Methods and Results) to ensure  
98 only a single gRNA integration event per cell, generating a CHO CRISPR knockout library  
99 for use in pooled screening (overview in Figure 1).

100

## 101 **Glutamine screening**

102 Glutamine is key to cell function and thus an important media component for animal  
103 cell culture media formulations<sup>25</sup>. However, glutamine is often oversupplied, and its  
104 catabolism produces ammonia, a toxic byproduct that negatively impacts cell growth,  
105 production, and product quality<sup>5,26–28</sup>. Understandably, it is of interest to identify engineering  
106 strategies that permit improved cell behavior in glutamine-free conditions. We thus screened  
107 the CHO CRISPR knockout library cells for growth in media with and without glutamine for

108 fourteen days. The cells were passaged every three days (growth profile in Supplementary  
109 Figure S1) and  $30 \times 10^6$  cells were collected at the beginning and the end of the screen for  
110 analysis to ensure adequate coverage.

111

### 112 **The gRNA library is well represented at the start of screening**

113 To ensure that all possible gene knockouts are screened it is important to verify that  
114 the gRNA library is well represented at the beginning of the screen. We therefore sampled the  
115 cells just prior to glutamine deprivation (T0) and sequenced the gRNAs present in the starting  
116 cell pool. From the entire library, only 2 genes (<0.1%) and 638 gRNAs (<4%) were absent  
117 at the initial time point. In all samples, median-normalized gRNA and gene sequencing depth  
118 was greater than 35 and 360 CPM (counts per million), respectively (Figure 2). Thus, the  
119 majority of the library was well represented before the CRISPR knockout library was subjected  
120 to screening.

121

### 122 **Glutamine screening reveals expected and novel targets**

123 To identify gRNAs impacting CHO cell growth in glutamine free media, we analyzed  
124 gRNA enrichment and depletion between samples grown for fourteen days in media with and  
125 without glutamine. As expected, the absence of glutamine does not display a strong selection  
126 pressure (Supplementary Figure S2), consistent with the ability of CHO cells to grow slowly  
127 in the absence of glutamine due to low levels of endogenous glutamine synthetase  
128 expression<sup>29</sup>. We found 20 genes (Figure 3) that were significantly enriched or depleted in all  
129 replicates. As expected, *Glul* (glutamine synthetase) gRNAs showed significant depletion in

130 cells grown without glutamine, consistent with its role as the enzyme responsible for *de novo*  
131 glutamine synthesis. Similarly, significant enrichment of *Gls* (glutaminase) gRNAs was  
132 observed, consistent with protection of the intracellular glutamine pool from undesirable  
133 catabolism when glutamine is not readily available.

134

### 135 **Disruption of *Abhd11* is conditionally beneficial dependent on presence of glutamine**

136 We found the strongest and most consistent gRNA enrichment in cells grown without  
137 glutamine was a poorly characterized putative lipase, *Abhd11*. We subsequently generated  
138 clonal *Abhd11* knockout cell lines using CRISPR-Cas9 and assessed their growth in media with  
139 and without glutamine. In accordance with the screen, knocking out *Abhd11* substantially  
140 improved growth in glutamine-free medium (Figure 4A) but also depressed growth in  
141 glutamine containing medium compared to control cells (Figure 4B).

142

143 *Abhd11* has been poorly studied and is currently annotated as a putative lipase.  
144 However, recent work reports that *Abhd11* associates with the alpha-ketoglutarate  
145 dehydrogenase complex ( $\alpha$ kgdhc) and prevents its de-lipoylation<sup>30</sup> (a crucial cofactor for its  
146 activity). The *Abhd11* knockout would thus be expected to decrease  $\alpha$ kgdhc activity. The  
147 benefit of the knockout in glutamine-free (and detriment in glutamine replete) conditions is  
148 congruous with this mechanism. In the presence of glutamine, wildtype cells fuel the TCA  
149 cycle heavily via glutaminolysis<sup>31</sup>, without *Abhd11*,  $\alpha$ kgdhc activity would be attenuated and  
150 entry of glutamine to the TCA cycle would be stunted. Consistent with this, we observe  
151 drastically increased glutamate secretion in KO cells when grown in media containing

152 glutamine (Figure 5) and decreased glutamine uptake (KO cultures maintain >3 mM glutamine  
153 at all timepoints while wildtype cells consume all glutamine by day 5 or 6, data not shown).

154

155 In the absence of glutamine, the decrease in  $\alpha$ kgdhc activity in knockout cells would  
156 act as an artificial bottleneck at alpha-ketoglutarate ( $\alpha$ kg), forcing carbon away from the TCA  
157 cycle and into glutamine biosynthesis. Thus, control cells, with functional *Abhd11*, would  
158 consume  $\alpha$ kg via  $\alpha$ kgdhc to a greater extent than knockout cells, pulling away from *de novo*  
159 glutamine synthesis, which is essential for growth in glutamine-free medium. Indeed, when  
160 cells are adapted via stepwise decreases in glutamine levels and directed evolution<sup>32</sup>, cells adapt  
161 by decreasing their expression of *Abhd11* (Supplementary Datafile 2). An overview of the  
162 putative impact of *Abhd11* on glutamine metabolism is shown in Figure 6.

163 To explore the relationship between *Abhd11* and glutamine metabolism, we further  
164 analyzed knockout and control cell lines and compared their transcriptomic profile when  
165 grown in media with and without glutamine (Supplementary Methods and Results).

166

## 167 **Discussion**

168 As CHO cells are the primary workhorse for the production of biopharmaceuticals,  
169 significant time and effort has been invested towards producing optimal cell lines for growth,  
170 high protein titer, and good protein quality. Here, we present a high-throughput approach to  
171 identify novel targets for CHO cell line engineering. The objective was two-fold: first to  
172 establish a CHO-specific metabolic CRISPR-Cas9 knockout screening platform in CHO cells  
173 and second to use this platform to explore CHO cell metabolism using an industrially relevant



174 screening setup. Glutamine is one of the major nutrients taken up by mammalian cells and  
175 plays an important role as an energy source in *in vitro* culture<sup>25,33</sup>. The fast consumption of  
176 glutamine results in accumulated ammonia in the medium, inhibiting cell growth, reducing  
177 productivity, and altering glycosylation patterns on heterologously expressed proteins<sup>5,27,34</sup>.  
178 While growth on glutamine-free media is possible, a significant decrease in growth rate is  
179 almost always observed<sup>35</sup>. It is therefore of interest to investigate genetic alterations that elicit  
180 a positive growth response to media lacking glutamine. We found several genes whose  
181 knockout resulted in a growth benefit in media without glutamine. Unsurprisingly, one of these  
182 genes was *Gls*, which codes for the primary glutamine-catabolizing enzyme. Many of the  
183 remaining targets found were novel with respect to their protective role in glutamine depletion  
184 in CHO cells and their roles in a biological context are a topic for further investigation. We  
185 chose to follow up on *Abhd11*, a gene with no clear link to glutamine metabolism that showed  
186 the most marked enrichment of gRNAs in cells grown under glutamine depleted compared to  
187 glutamine replete conditions. Our results are consistent with recent evidence linking *Abhd11*  
188 with a protective role of  $\alpha$ kgdhc in the TCA cycle<sup>36</sup>. We observed depressed growth of *Abhd11*  
189 knockout cells in glutamine containing media alongside glutamate accumulation in the media  
190 and lack of complete glutamine consumption. As glutamate (via glutaminolysis) is a major  
191 source of TCA cycle intermediates<sup>31</sup>, the secretion of glutamate (and assumed decrease in TCA  
192 cycle activity) is consistent with the observed reduced growth rate. Conversely, in glutamine  
193 free media, *Abhd11* knockout cells exhibited improved growth compared to the wild type cells.  
194 We postulate that the inhibition of  $\alpha$ -ketoglutarate catabolism leads to accumulation of  $\alpha$ -

195 ketoglutarate and increases its availability for conversion to glutamate and subsequently to  
196 glutamine, leading to better growth.

197 High-throughput CRISPR-Cas9 screening presents a novel approach to conduct  
198 forward genetic engineering and can provide an abundance of knowledge in the study of  
199 genotype to phenotype relationships. Over recent years CRISPR-Cas9 screens have been  
200 applied to a variety of mammalian cell types to study biological function<sup>20,21,37</sup>. Since the  
201 publication of initial CRISPR-Cas9 screens, comprehensive reviews and extensive method  
202 articles have been published<sup>38-40</sup>. We show here that CRISPR screening techniques can be  
203 applied to the industrially relevant CHO cell line. This approach enables a wide array of studies  
204 in CHO cells by applying different screening conditions or exploiting the existing variations  
205 of the Cas protein, such as catalytically inactive Cas9 coupled to transcriptional activators and  
206 repressors, for activation or repression screens as has shown potential in other mammalian  
207 cells<sup>39,41-45</sup>. With continuous advances in CRISPR screen design and comprehensive  
208 annotation of the CHO cell genome these types of screens will enable a new era of targeted  
209 engineering to improve CHO cell phenotypes.

210

## 211 **Methods**

### 212 **Plasmid design and construction**

213 The GFP\_2A\_Cas9 plasmid was constructed as previously described<sup>46</sup>. A Cas9  
214 expression vector for generation of a Cas9 expressing CHO cell line (from here on be referred  
215 to as CHO-S<sup>Cas9</sup>), was constructed by cloning the 2A peptide-linked Cas9 ORF from the  
216 GFP\_2A\_Cas9 expression vector<sup>46</sup> into a pcDNA<sup>TM</sup>3.1(+) vector (Thermo Fisher Scientific)

217 between the HindIII and BamHI sites. The construct will from here on be referred to as  
218 pcCas9. gRNA vectors were constructed using Uracil-Specific Excision Reagent (USER)  
219 friendly cloning as previously described<sup>47</sup>. Plasmids were purified using NucleoBond Xtra Midi  
220 EF (Macherey-Nagel) according to manufacturer's protocol. Target sequences and gRNA  
221 oligos are listed in Supplementary Table S2.

222

### 223 **Cell culture**

224 CHO-S wild type cells from Life Technologies were cultivated in CD-CHO medium  
225 (Thermo Fisher Scientific) supplemented with 8 mM L-Glutamine and 2  $\mu$ L/mL  
226 AntiClumping Agent (AC) (Thermo Fisher Scientific) in a humidified incubator at 37 °C, 5 %  
227 CO<sub>2</sub> at 120 RPM shake in sterile Corning® Erlenmeyer culture flasks (Sigma-Aldrich) unless  
228 otherwise stated. Viable cell density (VCD) was measured using the NucleoCounter®  
229 NC200™ (Chemometec) utilizing fluorescent dyes acridine orange and 4',6-diamidino-  
230 2phenylindole (DAPI) for the detection of total and dead cells. Cells were seeded at 0.3 x 10<sup>6</sup>  
231 cells/mL every three days or 0.5 x 10<sup>6</sup> cells every two days.

232

### 233 **Transfection and cell line generation**

234 For all transfections, CHO-S wild type cells at a concentration of 1 x 10<sup>6</sup> cells/mL in a  
235 six well plate (BD Biosciences) in AC free media were transfected with a total of 3.75  $\mu$ g DNA  
236 using FreeStyle™ MAX reagent together with OptiPRO SFM medium (Life Technologies)  
237 according to the manufacturer's instructions. For generation of CHO-S<sup>Cas9</sup>, CHO-S wild type  
238 cells were transfected with pcCas9. Stable cell pools were generated by seeding transfected

239 cells at  $0.2 \times 10^6$  cells/mL in 3 mL selection media containing 500  $\mu\text{g}/\text{mL}$  G418  
240 (SigmaAldrich) in CELLSTAR® 6 well Advanced TC plates (Greiner Bio-one) two days post  
241 transfection. Medium was changed every four days during selection. After two weeks of  
242 selection, cells were detached and adapted to grow in suspension. The clonal cell lines were  
243 analysed by Celigo Cell Imaging Cytometer (Nexcelom Bioscience) based on the green  
244 fluorescence level using the mask (blue fluorescence representing individual cells stained with  
245 NucBlue™ Live ReadyProbes™ Reagent; Thermo Fisher Scientific) + target 1 (green  
246 fluorescence) application. For generating knockout cell lines of screen targets, CHO-S wild  
247 type cells were transfected with GFP\_2A\_Cas9 and appropriate gRNA expression vectors at  
248 a DNA ratio of 1:1 (w:w). Two days after transfection cells were single cell sorted using a  
249 FACSJazz (BD Bioscience), gating for GFP positive cell population as described previously<sup>46</sup>.  
250 Indels in targeted genes were verified by Next Generation Sequencing (NGS) as described  
251 previously<sup>46</sup>. Primers are listed in Supplementary Table S2. Three clones with a confirmed  
252 indel and two control clones without indels were and expanded to 30 mL media before they  
253 were frozen down at  $1 \times 10^7$  cells per vial in spent CD-CHO medium with 5 % DMSO (Sigma-  
254 Aldrich).

255

## 256 **Characterizing CHO-S<sup>Cas9</sup> functionality**

257 To characterize Cas9 functionality we transfected clonal CHO-S<sup>Cas9</sup> cells with a vector  
258 expressing gRNA against Mgat1 and verified indel generation on a pool level by NGS as  
259 described previously<sup>48</sup> (using gRNA oligo primers MGAT1\_gRNA\_fwd and  
260 MGAT1\_gRNA\_rev and NGS primers MGAT1\_miseq\_fwd and MGAT1\_miseq\_rev listed

261 in Supplementary Table S2). To analyze GFP expression, clonal cells were seeded in wells of  
262 a 96-well optical-bottom microplate (Greiner Bio-One) and identified GFP positive cells on  
263 the Celigo Cell Imaging Cytometer (Nexcelom Bioscience) using the green fluorescence  
264 channel. GFP negative gating was set on the basis of fluorescence emitted from CHO-S wild  
265 type cells.

266

### 267 **Library design and construction**

268 For design of the metabolic gRNA library, a list of metabolic genes was extracted from  
269 the CHO metabolic network reconstruction<sup>3</sup> along with a list of genes with metabolic GO  
270 terms in CHO and associated transcription factors. The gRNA templates were  
271 computationally designed using CRISPy (<http://crispy.biosustain.dtu.dk/>), resulting in a  
272 gRNA library with a minimum of 5 gRNAs per gene. The oligo library was synthesized by  
273 CustomArray. Full-length oligonucleotides were amplified by PCR using KAPA Hifi (Kapa  
274 Biosystems), size selected on a 2% agarose gel and purified with a QIAquick Gel Extraction  
275 Kit (Qiagen) as per manufacturer's protocol. The gRNA-LGP vector (Addgene #52963) was  
276 digested using BsmBI (New England BioLabs) (4  $\mu$ g gRNA-LGP vector, 5  $\mu$ L buffer 3.1, 5  
277  $\mu$ L 10 x BSA, 3  $\mu$ L BsmBI and H<sub>2</sub>O up to 50  $\mu$ L were mixed and incubated at 55°C for 3  
278 hours). Subsequently, 2  $\mu$ L of calf intestinal alkaline phosphatase (New England BioLabs) was  
279 added to the digested vector and the mix was incubated at 37°C for 30 minutes before it was  
280 purified with a QIAquick PCR Purification Kit (Qiagen) as per manufacturer's protocol. To  
281 assemble the gRNAs into the vector a 20  $\mu$ L Gibson ligation reaction (New England BioLabs)  
282 was carried out (25 ng linearized vector, 10 ng purified insert, 10  $\mu$ L 2 x Gibson Assembly

283 Master Mix (New England BioLabs) and up to 20  $\mu$ L H<sub>2</sub>O were mixed and incubated at 50°C  
284 for 1 hour). The assembled vector was purified using QIAquick PCR purification (Qiagen)  
285 and transformed into chemically competent E. coli (Invitrogen). Transformed bacteria were  
286 plated onto LB-carbenicillin plates for overnight incubation at 37°C, and plasmid DNA was  
287 purified using a HiSpeed Plasmid Maxi Kit (Qiagen).

288

### 289 **Lentiviral packaging**

290 To produce the lentivirus, HEK293T cells were cultivated in DMEM supplemented  
291 with 10% Fetal Bovine Serum (FBS). One day prior to transfection, cells were seeded in a  
292 15cm tissue culture plate at a density suitable for reaching 70-80% confluency at time of  
293 transfection. Culture medium was replaced with prewarmed DMEM containing 10% FBS. 36  
294  $\mu$ L Lipofectamine 3000 (Life Technologies) was diluted in 1.2 mL OptiMEM  
295 (LifeTechnologies) and in a separate tube 48  $\mu$ L P3000 reagent, 12  $\mu$ g pCMV (Addgene  
296 #12263), 3  $\mu$ g pMD2.G (Addgene #12259) and 9  $\mu$ g lentiviral vector were diluted in 1.2 mL  
297 OptiMEM. The solutions were incubated for 5 minutes at room temperature, mixed,  
298 incubated for another 30 minutes before they were added dropwise to the HEK293T cells. 48  
299 hours and 72 hours after transfection the viral particles were concentrated using Centricon  
300 Plus-20 Centrifugal ultrafilters (100 kDa pore size), aliquoted and stored at -80°C.

301

### 302 **Puromycin kill curve**

303 To determine the concentration of puromycin to be used to select the CHO library  
304 cells for gRNA insertion, a puromycin kill curve for CHO cells was determined. CHO-S wild

305 type cells at a concentration of  $1 \times 10^6$  cells/mL in media containing various amounts of  
306 puromycin (0, 0.25, 0.5, 1, 2, 3, 4, 5, 6, 7, 8 and 10  $\mu\text{g}/\text{mL}$ ). Cell viability and VCD was  
307 monitored over 7 days and based on halted growth and complete cell death of wild type cells  
308 10  $\mu\text{g}/\text{mL}$  was used for further experiments (Supplementary Figure S3).

309

### 310 **Transducing CHO-S<sup>Cas9</sup> with library virus**

311 CHO-S<sup>Cas9</sup> cells were seeded at  $0.3 \times 10^6$  cells/mL in 1 mL media in 26 wells of 12 well  
312 plates (BD Biosciences). In 25 of the wells, cells were transduced with 4  $\mu\text{L}$  library virus/well  
313 along with 8  $\mu\text{g}/\text{mL}$  Polybrene (Sigma-Aldrich) aiming for an MOI at 0.3-0.4 (Supplementary  
314 Methods and Results). Cells in the remaining well were left non-transduced as a negative  
315 control. After 24 hours, the cells were washed in PBS (Sigma-Aldrich) by centrifugation at 200  
316 x g, resuspended in media and seeded in a new 12 well plate. After 24 hours, cells were  
317 expanded to 3 mL media in wells of 6 well plates (BD Biosciences). Selection for cells  
318 containing the gRNA insert was initiated by adding 10  $\mu\text{g}/\text{mL}$  puromycin (Thermo Fisher  
319 Scientific) to each well (see puromycin kill curve in Supplementary Figure S3). Non-transduced  
320 control cells were monitored for complete cell death, equating finalised selection. The cells  
321 were washed and passed twice before they were expanded to attain enough cells to create a  
322 cell bank. Cells were frozen down at  $1 \times 10^7$  cells per vial in spent CD-CHO medium with 5  
323 % DMSO (SigmaAldrich) and will from here on be referred to as CHO-S<sup>Cas9</sup> library cells.

324

325

326

## 327 **Screening and DNA extraction**

328 CHO-SCas<sup>9</sup> library cells were thawed in 30 mL media and expanded to 60 mL before  
329 starting the screen. On day 0 (T<sub>0</sub>) 1.5 x 10<sup>7</sup> cells were spun down at 200 x g and resuspended  
330 in 60 mL appropriate screening media. The cells were grown for 14 days (passed to 0.25 x 10<sup>6</sup>  
331 cells/mL every third day). 30 x 10<sup>6</sup> cells were collected at T<sub>0</sub> and on day 14 (T<sub>14</sub>). The pellets  
332 were stored at -80°C until further use. gDNA extraction of all 30 x 10<sup>6</sup> cells was carried out  
333 using GeneJET Genomic DNA Purification Kit (Thermo Fisher Scientific) following the  
334 manufacturer's protocol. gDNA was eluted in 100 µL preheated elution buffer from the  
335 purification kit and incubated for 10 minutes before final centrifugation for maximum gDNA  
336 recovery.

337

## 338 **Preparation for next generation sequencing**

339 50 µL PCR reactions with 3 µg input gDNA per reaction were run using Phusion®  
340 Hot Start II High-Fidelity DNA Polymerase (Thermo Fisher Scientific) (95°C for 4 min; 30  
341 times: 98°C for 45s, 60°C for 30 s, 72°C for 1 min; 72°C for 7 min) using primers flanking the  
342 gRNA insert containing overhang sequenced compatible with Illumina Nextera XT indexing  
343 and 8 random nucleotides to increase the diversity of the sequences (LIB\_8xN\_NGS\_FWD  
344 and LIB\_8xN\_NGS\_REV listed in Supplemental Table S2). Double size selection was  
345 performed using Agencourt AMPure XP beads (Beckman Coulter) to exclude primer dimers  
346 and genomic DNA. The amplicons were indexed using Nextera XT Index Kit v2 (Illumina)  
347 sequence adapters using KAPA HiFi HotStart ReadyMix (KAPA Biosystems) (95°C for 3 min;  
348 8 times: 95°C for 30s, 55°C for 30 s, 72°C for 30 s; 72°C for 5 min) and subjected to a second



349 round of bead-based size exclusion. The resulting library was quantified with Qubit® using  
350 the dsDNA HS Assay Kit (Thermo Fisher Scientific) and the fragment size was determined  
351 using a 2100 Bioanalyzer Instrument (Agilent) before running the samples on a NextSeq 500  
352 sequencer (Illumina).

353

## 354 **Analysis**

355 Raw FASTQ files for samples from the end time points of glutamine selection were  
356 uploaded to PinAPL-PY (<http://pinapl-py.ucsd.edu/>)<sup>49</sup> along with a file containing the  
357 sequences for all gRNAs contained in the library. Top candidates for enriched and for depleted  
358 gRNAs were ranked by an adjusted robust rank aggregation (aRRA) method<sup>50</sup> and filtered for  
359 significance, compared between the replicates and used for verification of the screen. The  
360 screen was analyzed using default parameters set by PinAPL-PY.

361

## 362 **Batch culture**

363 *Abbd11* knockout cell lines were seeded at  $0.3 \times 10^6$  cells/mL in 90 mL CD-CHO media  
364 with and without glutamine supplemented with 1  $\mu$ L/mL AC in 250 mL Corning® Erlenmeyer  
365 culture flasks (Sigma-Aldrich). Cell viability and density were measured every day for a  
366 maximum of fourteen days.

367

## 368 **Analysis of cell line adapted to absence of glutamine by directed evolution**

369 A previously established cell line that was adapted to grow without glutamine by  
370 stepwise decrease in glutamine concentration and directed evolution<sup>32</sup> was grown in batch

371 culture as previously described<sup>51</sup>. Samples were taken at the same time points and analysed  
372 using a mouse Agilent 22 k microarray (G4121B) platform as described for the parental cell  
373 line grown in medium with 8mM glutamine<sup>51</sup>. Differential transcriptome and statistical  
374 analyses were performed as previously described<sup>51</sup>.

375

## 376 **Acknowledgements**

377 The authors wish to thank Nachon Charayanonda Petersen for assistance, cell line  
378 generation and batch culture and Anna Koza, Alexandra Hoffmeyer, Pannipa Pornpitapong  
379 for assistance with NGS, Dr. Prashant Mali for packaging the gRNA library into the lentivirus,  
380 Dr. James A Nathan for discussions regarding *Abbd11* and Daria Sergeeva for co-drawing  
381 Figure 1. This work was supported by the Novo Nordisk Foundation (NNF10CC1016517  
382 and NNF16OC0021638) and NIGMS (R35 GM119850, NEL).

383

384

385

386

387

388

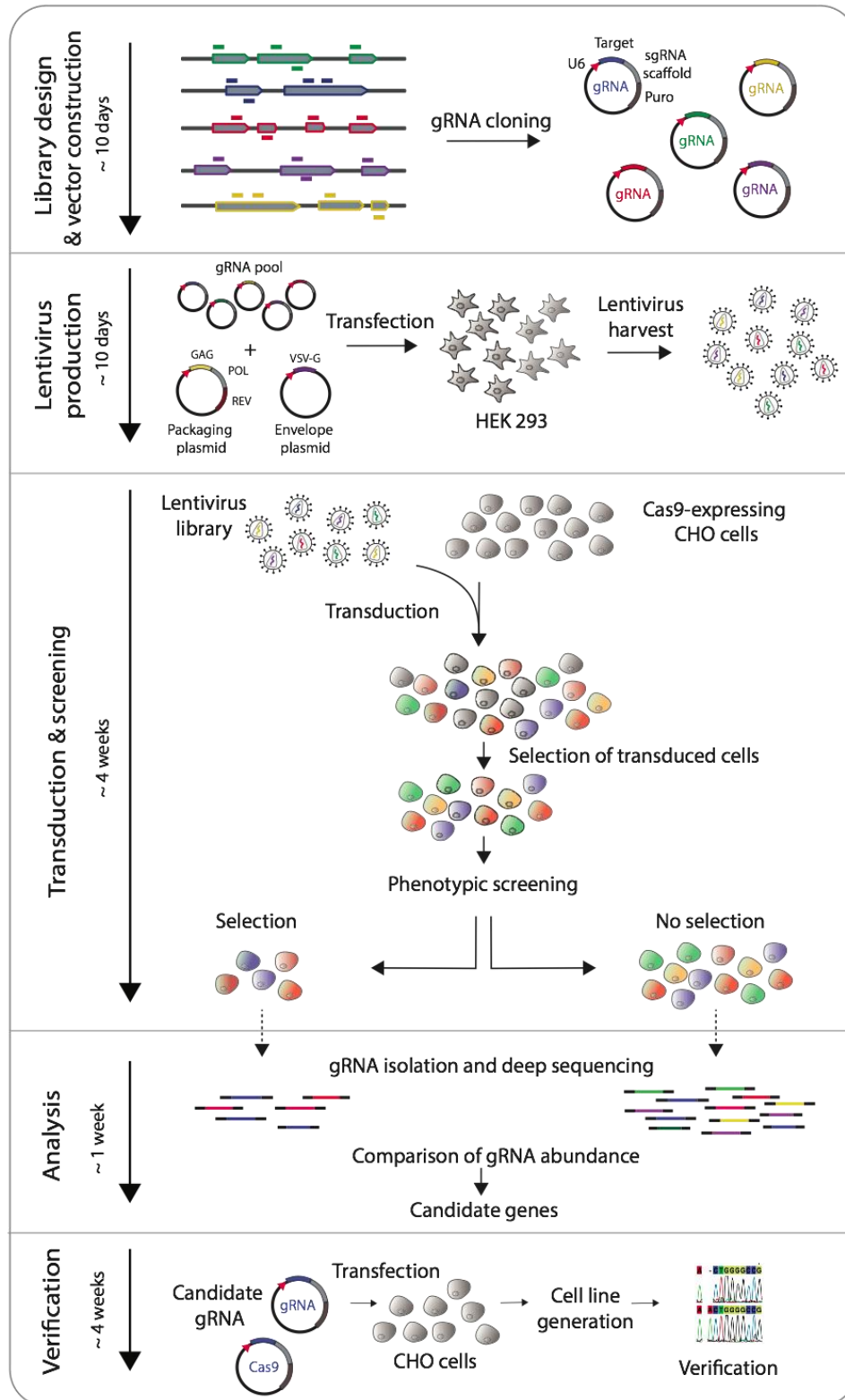
389

390

391

392

393 **Figures**



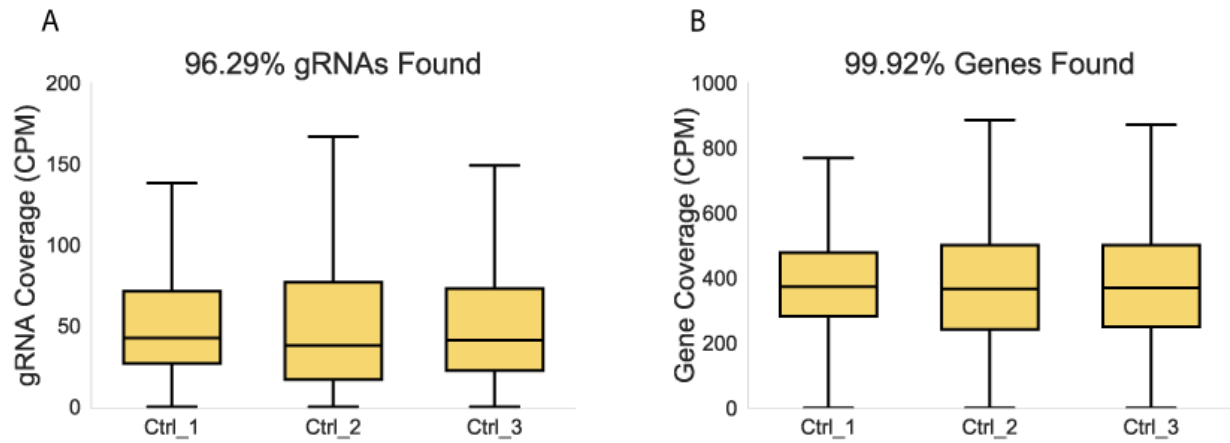
394

395 **Figure 1 Screening overview**

396 gRNAs are computationally designed to target the genes of interest, then synthesized and cloned into gRNA  
397 scaffold containing vectors. HEK cells are transfected with packaging vectors and gRNA vectors to generate a  
398 pool of viruses containing all the gRNA vectors. After harvest, the pooled library is used to transduce Cas9-  
399 expressing CHO cells at a low MOI to ensure a single integration event per cell. Cells positive for gRNA  
400 integration are selected for with antibiotics before undergoing a phenotypic screen. Genomic DNA is extracted  
401 from the collected cells and gRNA presence is compared between samples. Enriched or depleted gRNAs are  
402 ranked and candidate genes are phenotypically validated.

403

404



405

406 **Figure 2 Screen verification**

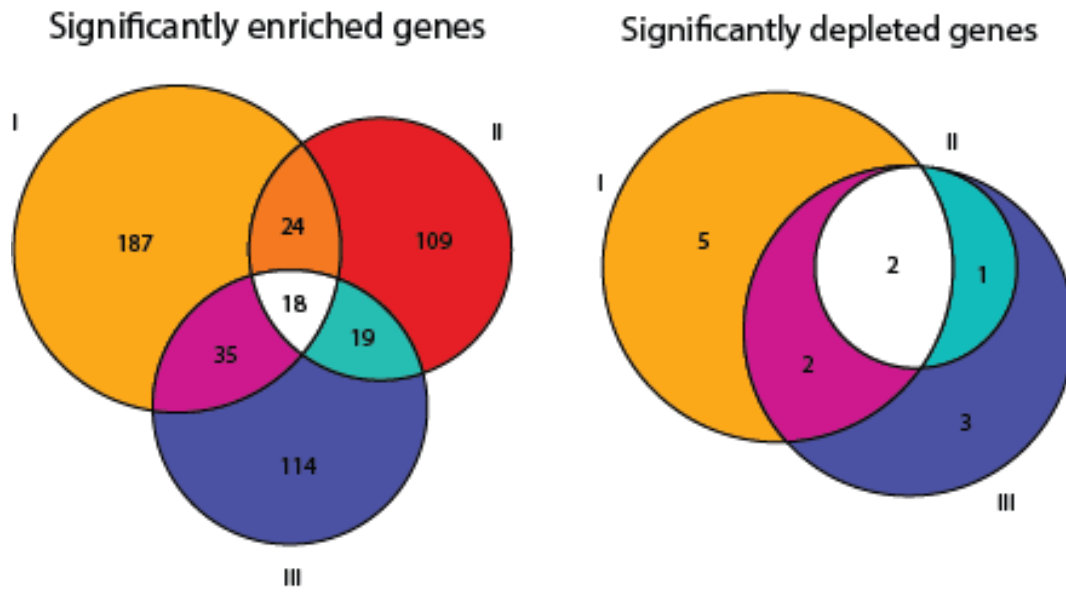
407 A) Read count per gRNA. B) Total read count per gene (summed over all gRNAs). Shown are normalized read  
408 counts (counts per million/CPM) for three replicate experiments prior to starting selection. Outliers not  
409 displayed.

410

411

412

413



414

415

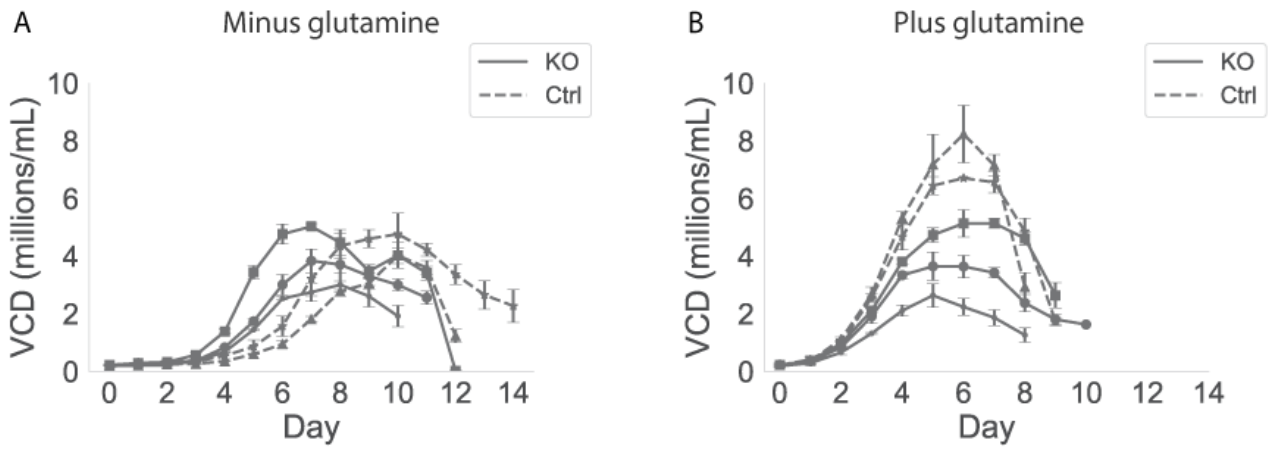
416 **Figure 3 Significantly enriched and depleted genes following glutamine selection**

417 Three glutamine screens of the knockout library were carried out and the significantly depleted and enriched  
418 genes from each replicate are shown. While there was variability between replicates (I-III), eighteen significantly  
419 enriched genes and two significantly depleted genes were commonly observed in all experiments.

420

421

422



423

424 **Figure 4 Growth curves for *Abhd11* knockout and control cell lines in batch culture in media without**  
425 **and with glutamine**

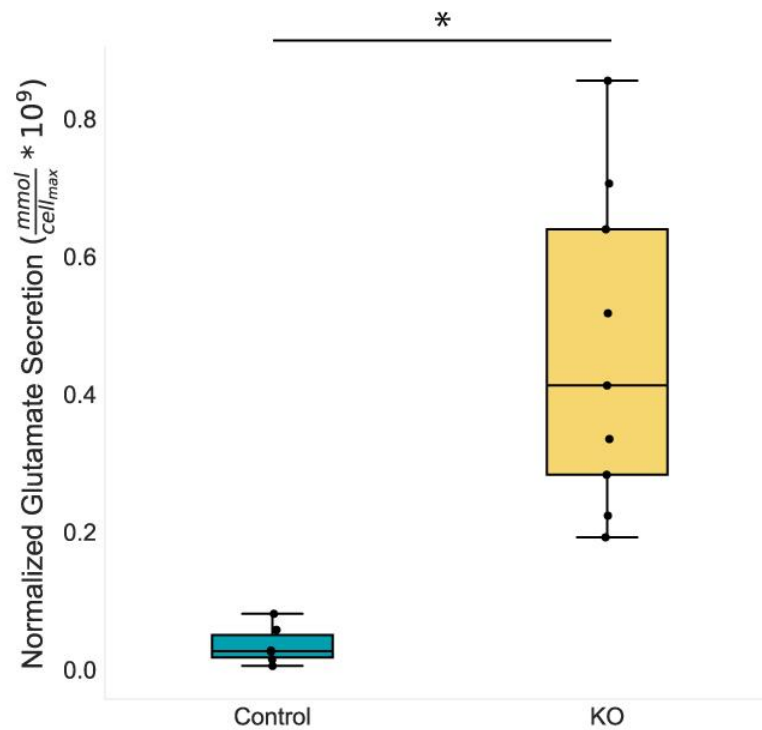
426 Growth curves for three *Abhd11* knockout (KO) and two control (Ctrl) cell lines grown in three replicates in  
427 media without glutamine (A) and with glutamine (B). Viable cell density (VCD) was measured every day over a  
428 period of 14 days.

429

430

431

432



433

434 **Figure 5 Impact of *Abhd11* knockout on glutamate secretion**

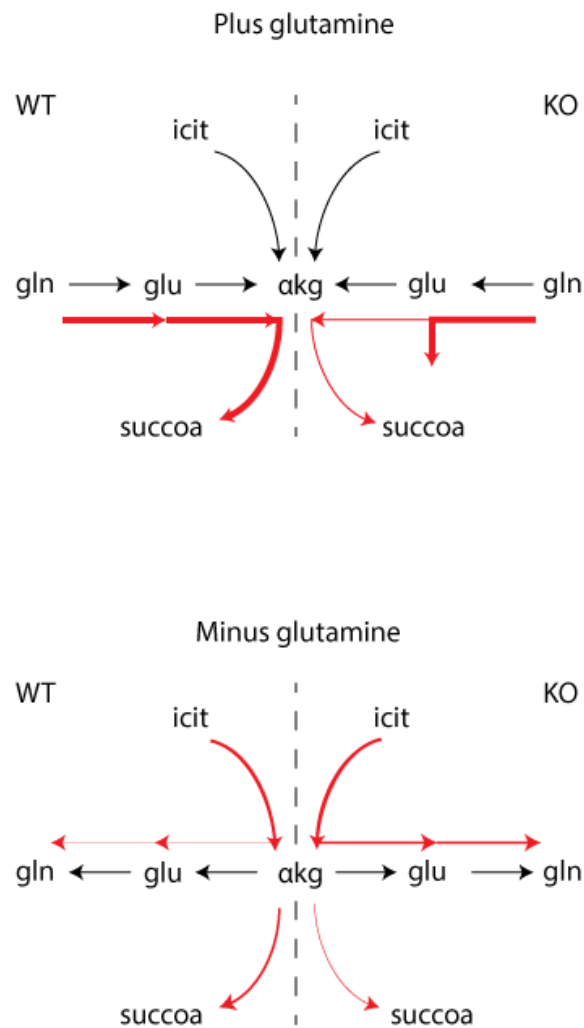
435 Wild type (control) and knockout cells were grown in glutamine replete conditions. Glutamate secreted during  
436 the growth phase (e.g., until maximum VCD was reached) was normalized by the maximum VCD to  
437 approximate cell specific glutamate secretion. Knockout cells secreted significantly more glutamate than  
438 wildtype cells. \* indicates a statistically significant difference ( $p < 0.05$ ) as calculated by a two-tailed Welch's t-  
439 test.

440

441

442





443

444

445 **Figure 6 Putative mechanism of action for wild type (WT) and *Abhd11* knockout (KO) cells grown in**  
446 **media with or without glutamine.**

447 *Abhd11* associates with and protects the  $\alpha$ kgdhc. (a) In the presence of gln, cells fuel the TCA cycle through

448 gln catabolism. In *Abhd11* KO cell lines,  $\alpha$ kgdhc flux (and TCA cycle activity) is decreased,  $\alpha$ kg and glu

449 accumulate, and glu is secreted, leading to decreased growth for KO cells. (b) Without gln, the TCA cycle is

450 largely fueled through glycolysis. In *Abhd11* KO cell lines, the decrease in  $\alpha$ kgdhc activity leads to increased

451  $\alpha$ kg, which permits increased flux to glu and *de novo* glutamine synthesis. With normal *Abhd11* function, cells

452 do not have this bottleneck and  $\alpha$ kgdhc activity competes more strongly with gln biosynthesis, leading to

453 decreased growth for WT cells.  $\alpha$ kgdhc: alpha ketoglutarate complex, icit: isocitrate,  $\alpha$ kg: alpha-ketoglutarate,

454 succoa: succinyl coenzyme A, gln: glutamine, glu: glutamate.

455

## 456   **References**

- 457   1.   Walsh, G. Biopharmaceutical benchmarks 2018. *Nat. Biotechnol.* **36**, 1136–1145 (2018).
- 458   2.   Jayapal, K. P., Wlaschin, K. F., Hu, W. S. & Yap, M. G. S. Recombinant Protein Therapeutics from  
459       CHO Cells — 20 Years and Counting. *Chemical Engineering Progress* vol. 103 40–47 (2007).
- 460   3.   Hefzi, H. *et al.* A Consensus Genome-scale Reconstruction of Chinese Hamster Ovary Cell  
461       Metabolism. *Cell Syst* **3**, 434–443.e8 (2016).
- 462   4.   Zielinski, D. C. *et al.* Systems biology analysis of drivers underlying hallmarks of cancer cell metabolism.  
463       *Sci. Rep.* **7**, 41241 (2017).
- 464   5.   Yang, M. & Butler, M. Effects of ammonia on CHO cell growth, erythropoietin production, and  
465       glycosylation. *Biotechnol. Bioeng.* **68**, 370–380 (2000).
- 466   6.   Hansen, H. A. & Emborg, C. Influence of ammonium on growth, metabolism, and productivity of a  
467       continuous suspension Chinese hamster ovary cell culture. *Biotechnol. Prog.* **10**, 121–124 (1994).
- 468   7.   Hassell, T., Gleave, S. & Butler, M. Growth inhibition in animal cell culture. The effect of lactate and  
469       ammonia. *Appl. Biochem. Biotechnol.* **30**, 29–41 (1991).
- 470   8.   Ozturk, S. S., Riley, M. R. & Palsson, B. O. Effects of ammonia and lactate on hybridoma growth,  
471       metabolism, and antibody production. *Biotechnol. Bioeng.* **39**, 418–431 (1992).
- 472   9.   Brinkrolf, K. *et al.* Chinese hamster genome sequenced from sorted chromosomes. *Nat. Biotechnol.* **31**,  
473       694–695 (2013).
- 474   10.   Lewis, N. E. *et al.* Genomic landscapes of Chinese hamster ovary cell lines as revealed by the *Cricetulus*  
475       *griseus* draft genome. *Nat. Biotechnol.* **31**, 759–765 (2013).
- 476   11.   Xu, X. *et al.* The genomic sequence of the Chinese hamster ovary (CHO)-K1 cell line. *Nat. Biotechnol.*  
477       **29**, 735–741 (2011).
- 478   12.   Gutierrez, J. M. & Lewis, N. E. Optimizing eukaryotic cell hosts for protein production through  
479       systems biotechnology and genome-scale modeling. *Biotechnol. J.* **10**, 939–949 (2015).
- 480   13.   Santiago, Y. *et al.* Targeted gene knockout in mammalian cells by using engineered zinc-finger

- 481 nucleases. *Proc. Natl. Acad. Sci. U. S. A.* **105**, 5809–5814 (2008).
- 482 14. Sakuma, T. *et al.* Homologous Recombination-Independent Large Gene Cassette Knock-in in CHO  
483 Cells Using TALEN and MMEJ-Directed Donor Plasmids. *Int. J. Mol. Sci.* **16**, 23849–23866 (2015).
- 484 15. Cullen, L. M. & Arndt, G. M. Genome-wide screening for gene function using RNAi in mammalian  
485 cells. *Immunol. Cell Biol.* **83**, 217–223 (2005).
- 486 16. Klanert, G. *et al.* A cross-species whole genome siRNA screen in suspension-cultured Chinese hamster  
487 ovary cells identifies novel engineering targets. *Sci. Rep.* **9**, 8689 (2019).
- 488 17. Smith, I. *et al.* Evaluation of RNAi and CRISPR technologies by large-scale gene expression profiling in  
489 the Connectivity Map. *PLoS Biol.* **15**, e2003213 (2017).
- 490 18. Kaelin, W. G., Jr. Molecular biology. Use and abuse of RNAi to study mammalian gene function. *Science*  
491 **337**, 421–422 (2012).
- 492 19. Hart, T., Brown, K. R., Sircoulomb, F., Rottapel, R. & Moffat, J. Measuring error rates in genomic  
493 perturbation screens: gold standards for human functional genomics. *Mol. Syst. Biol.* **10**, 733 (2014).
- 494 20. Koike-Yusa, H., Li, Y., Tan, E.-P., Velasco-Herrera, M. D. C. & Yusa, K. Genome-wide recessive  
495 genetic screening in mammalian cells with a lentiviral CRISPR-guide RNA library. *Nat. Biotechnol.* **32**,  
496 267–273 (2014).
- 497 21. Shalem, O. *et al.* Genome-scale CRISPR-Cas9 knockout screening in human cells. *Science* **343**, 84–87  
498 (2014).
- 499 22. Zhou, Y. *et al.* High-throughput screening of a CRISPR/Cas9 library for functional genomics in human  
500 cells. *Nature* **509**, 487–491 (2014).
- 501 23. Bassett, A. R., Kong, L. & Liu, J.-L. A genome-wide CRISPR library for high-throughput genetic  
502 screening in *Drosophila* cells. *J. Genet. Genomics* **42**, 301–309 (2015).
- 503 24. Krämer, A., Green, J., Pollard, J., Jr & Tugendreich, S. Causal analysis approaches in Ingenuity Pathway  
504 Analysis. *Bioinformatics* **30**, 523–530 (2014).
- 505 25. Yao, T. & Asayama, Y. Animal-cell culture media: History, characteristics, and current issues. *Reprod.*  
506 *Med. Biol.* **16**, 99–117 (2017).

- 507 26. Borys, M. C., Linzer, D. I. & Papoutsakis, E. T. Ammonia affects the glycosylation patterns of  
508 recombinant mouse placental lactogen-I by chinese hamster ovary cells in a pH-dependent manner.  
509 *Biotechnol. Bioeng.* **43**, 505–514 (1994).
- 510 27. Thorens, B. & Vassalli, P. Chloroquine and ammonium chloride prevent terminal glycosylation of  
511 immunoglobulins in plasma cells without affecting secretion. *Nature* **321**, 618–620 (1986).
- 512 28. Taschwer, M. *et al.* Growth, productivity and protein glycosylation in a CHO EpoFc producer cell line  
513 adapted to glutamine-free growth. *Journal of Biotechnology* vol. 157 295–303 (2012).
- 514 29. Fan, L. *et al.* Improving the efficiency of CHO cell line generation using glutamine synthetase gene  
515 knockout cells. *Biotechnol. Bioeng.* **109**, 1007–1015 (2012).
- 516 30. Bailey, P. S. J. *et al.* ABHD11 regulates 2-oxoglutarate abundance by protecting mitochondrial lipoylated  
517 proteins from lipid peroxidation damage. *bioRxiv* doi:10.1101/2020.04.18.048082.
- 518 31. Ahn, W. S. & Antoniewicz, M. R. Parallel labeling experiments with [1,2-(13)C]glucose and [U-  
519 (13)C]glutamine provide new insights into CHO cell metabolism. *Metab. Eng.* **15**, 34–47 (2013).
- 520 32. Bort, J. A. H., Hernández Bort, J. A., Stern, B. & Borth, N. CHO-K1 host cells adapted to growth in  
521 glutamine-free medium by FACS-assisted evolution. *Biotechnology Journal* vol. 5 1090–1097 (2010).
- 522 33. Newsholme, P. *et al.* Glutamine and glutamate as vital metabolites. *Braz. J. Med. Biol. Res.* **36**, 153–163  
523 (2003).
- 524 34. Yang, M. & Butler, M. Effect of ammonia on the glycosylation of human recombinant erythropoietin in  
525 culture. *Biotechnol. Prog.* **16**, 751–759 (2000).
- 526 35. Altamirano, C., Paredes, C., Cairo, J. J. & Godia, F. Improvement of CHO Cell Culture Medium  
527 Formulation: Simultaneous Substitution of Glucose and Glutamine. *Biotechnol. Prog.* **16**, 69–75 (2000).
- 528 36. Bailey, P. S. J., Ortmann, B. M., Costa, A. S., Frezza, C. & Nathan, J. A. T6 Identification of ROLIP as  
529 a mitochondrial regulator of metabolism and the hypoxia response pathway. *BTS/ BALR/ BLF Early*  
530 *Career Investigator Awards Symposium* (2019) doi:10.1136/thorax-2019-btsabstracts2019.6.
- 531 37. Wang, T., Wei, J. J., Sabatini, D. M. & Lander, E. S. Genetic Screens in Human Cells Using the  
532 CRISPR-Cas9 System. *Science* **343**, 80–84 (2014).

- 533 38. Schuster, A. *et al.* RNAi/CRISPR Screens: from a Pool to a Valid Hit. *Trends Biotechnol.* **37**, 38–55  
534 (2019).
- 535 39. Joung, J. *et al.* Genome-scale CRISPR-Cas9 knockout and transcriptional activation screening. *Nat.*  
536 *Protoc.* **12**, 828–863 (2017).
- 537 40. Doench, J. G. Am I ready for CRISPR? A user’s guide to genetic screens. *Nat. Rev. Genet.* **19**, 67–80  
538 (2017).
- 539 41. Gilbert, L. A. *et al.* Genome-Scale CRISPR-Mediated Control of Gene Repression and Activation. *Cell*  
540 **159**, 647–661 (2014).
- 541 42. Joung, J. *et al.* Genome-scale activation screen identifies a lncRNA locus regulating a gene  
542 neighbourhood. *Nature* **548**, 343–346 (2017).
- 543 43. Heaton, B. E. *et al.* A CRISPR Activation Screen Identifies a Pan-avian Influenza Virus Inhibitory Host  
544 Factor. *Cell Rep.* **20**, 1503–1512 (2017).
- 545 44. Liu, S. J. *et al.* CRISPRi-based genome-scale identification of functional long noncoding RNA loci in  
546 human cells. *Science* **355**, (2017).
- 547 45. Rosenbluh, J. *et al.* Complementary information derived from CRISPR Cas9 mediated gene deletion  
548 and suppression. *Nat. Commun.* **8**, 15403 (2017).
- 549 46. Grav, L. M. *et al.* One-step generation of triple knockout CHO cell lines using CRISPR/Cas9 and  
550 fluorescent enrichment. *Biotechnol. J.* **10**, 1446–1456 (2015).
- 551 47. Ronda, C. *et al.* Accelerating genome editing in CHO cells using CRISPR Cas9 and CRISPy, a web-  
552 based target finding tool. *Biotechnol. Bioeng.* **111**, 1604–1616 (2014).
- 553 48. Lee, J. S., Kallehauge, T. B., Pedersen, L. E. & Kildegaard, H. F. Site-specific integration in CHO cells  
554 mediated by CRISPR/Cas9 and homology-directed DNA repair pathway. *Sci. Rep.* **5**, 8572 (2015).
- 555 49. Spahn, P. N. *et al.* PinAPL-Py: A comprehensive web-application for the analysis of CRISPR/Cas9  
556 screens. *Sci. Rep.* **7**, 15854 (2017).
- 557 50. Li, W. *et al.* MAGeCK enables robust identification of essential genes from genome-scale  
558 CRISPR/Cas9 knockout screens. *Genome Biol.* **15**, 554 (2014).

- 559 51. Hernández Bort, J. A. *et al.* Dynamic mRNA and miRNA profiling of CHO-K1 suspension cell  
560 cultures. *Biotechnol. J.* **7**, 500–515 (2012).